



Technical Notes

Simulation study of energy resolution of the high-pressure xenon gamma-ray spectrometer



Jinchao Ma^a, Pin Gong^{a,b}, Xiaobin Tang^{a,b,*}, Peng Wang^c, Wen Yan^a, Dajian Liang^d, Zeyu Wang^d, Rui Zhang^a, Xiaolei Shen^a

^a Department of Nuclear Science and Technology, Nanjing University of Aeronautics and Astronautics, Nanjing 210016, China

^b Key Laboratory of Nuclear Technology Application and Radiation Protection in Astronautics, Ministry of Industry and Information Technology, Nanjing, 211106, China

^c School of Environmental and Biological Engineering, Nanjing University of Science and Technology, Nanjing 210094, China

^d Joint Laboratory of Nuclear Technology and Artificial Intelligence, Nanjing University of Aeronautics and Astronautics, Nanjing 210016, China

ARTICLE INFO

Keywords:

Energy resolution
High-pressure xenon detector
Modeling
Garfield++

ABSTRACT

High-pressure xenon (HPXe) ionization chamber is a high-energy-resolution radiation detector for gamma spectrometry with excellent physical properties. It has a wide range of operation temperatures, excellent radiation resistance, and long-life performance. Energy resolution is an important parameter of an HPXe gamma-ray spectrometer and has been investigated by scientists through experimental methods for years. However, in previous researches, there are few simulations on energy resolution of different ionization chamber structures. In this paper, three simulation tools are used to simulate the energy resolution of the HPXe spectrometer. Monte Carlo simulation software PHITS and finite element analysis software ANSYS are used to establish the model of the HPXe ionization chamber with a shielding grid. Garfield++ is adopted to obtain the output signal for analyzing the energy resolution. The energy resolution under different gas components and shielding grid structures are simulated. Results show that when the gamma-ray energy is 662 keV, the deviation between the simulated energy resolution obtained in this paper and the expected theoretical value 0.6% reported in the document Dmitrenko et al. (1986) is 13.05%. Besides, the experimental energy resolution of the HPXe gamma-ray spectrometer made by MEPHI (Dmitrenko et al., 2008) is about 2% at 662keV. Therefore, the value of simulated result in this paper is between the experimental result of MEPHI and the theoretical value, and closer to the theoretical value, which means that the simulation method proposed in this paper has high credibility.

1. Introduction

High-pressure xenon (HPXe) gamma-ray spectrometer has been used for gamma-ray detection for decades. This kind spectroscopic detector has various advantages: (a) good energy resolution ($\sim 2.0\%$ at 662 keV) which is close to that of HPGe, but without cryogenic system, (b) applicability in harsh high-radiation environments, (c) broad operating temperature range (10–180 °C), and (d) high stability and capability for long term working [1]. Since the energy resolution is the most critical performance parameter of HPXe gamma-ray spectrometers, there are many researchers focusing on the improvement of this parameter for many years [2,3]. However, despite many years of research, the experimental energy resolution is still far from its expected theoretical limit of $\sim 0.6\%$ at 662 keV [4]. Meanwhile, due to the complex technology of manufacturing, and the limited experimental research, the design and energy resolution of HPXe spectrometer has

not improved considerably since the 1990s. Conducting a study by simulation is easier than by experiment. However, several parameters of the HPXe detector which have been proven to affect the energy resolution seriously, such as gas density, electric field distribution [5], and geometry of shielding grid [6], have not been fully studied in the previous simulations. The development of a simulation method or process that can directly associate the design parameters and energy resolution performance of the HPXe gamma-ray spectrometer will provide a further convenient way to design the HPXe spectrometer with excellent performance.

In this paper, an approach of combining three simulation tools, named Garfield++, ANSYS, and PHITS, was proposed to establish the relationship between the design parameters and energy resolution of the HPXe detector. The effects of the different parameters on the energy resolution will be discussed later.

* Corresponding author at: Department of Nuclear Science and Technology, Nanjing University of Aeronautics and Astronautics, Nanjing 210016, China.
E-mail address: tangxiaobin@nuaa.edu.cn (X. Tang).

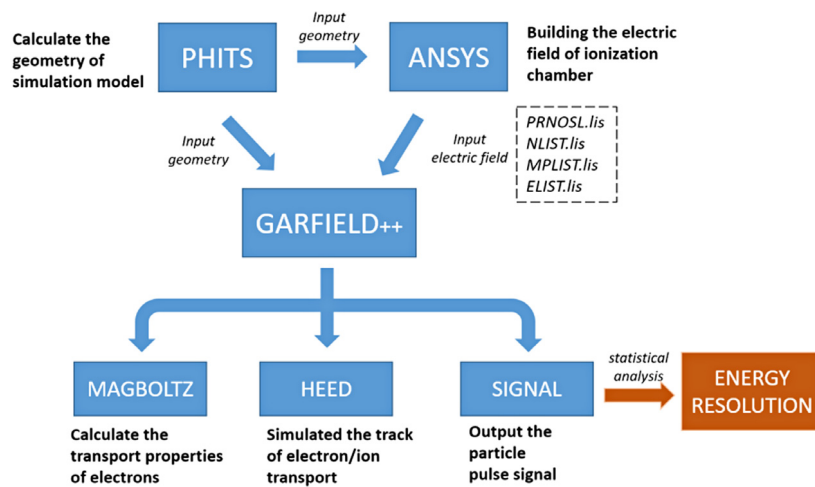


Fig. 1. Overview of the adopted tools and programs and their interplay.

2. Principle and method

2.1. Simulation method

Three simulation tools used in this paper have different functions. The Monte Carlo simulation software PHITS [7,8] is used to establish the geometry of the detector. The finite element analysis programs ANSYS [9] is used to calculate electric field distribution in the detector. Garfield++ is an open-source toolkit developed by the European Organization for Nuclear Research (CERN) for the detailed simulation of particle detectors that use a gas mixture or semiconductor material as a sensitive medium [10]. This toolkit has three subprograms, namely, “Magboltz”, “Heed”, and “Signals”. “Magboltz” is a program for calculating the transport properties of electrons in gas mixtures. “Heed” is a program for simulating the ionization pattern produced along the track of relativistic charged particles. In addition, “Heed” is an implementation of the photo-absorption ionization (PAI) model, and it can only reflect the photoelectric effect (including escape peak). Other interactions of gamma quanta with matter (like Compton) cannot be simulated in Garfield++. “Signal” is a program for calculating the induced signals on the anode of the chamber on the basis of the Shockley–Ramo theorem. The amplitudes of the signals obtained by Garfield++ are used to calculate energy resolution. The overview of the different tools and programs used in the approach is shown in Fig. 1.

The simulation process can be divided into the following three parts:

- (1) Preliminary establishing the geometrical structure by PHITS: First, the wall thickness of the detector was determined on the basis of the minimum detectable gamma-ray energy. Then, the diameter of the detector was calculated on the basis of the gas pressure and the wall thickness. After the diameter of the ionization chamber was determined, the spatial distribution of the energy deposition in the ionization chamber was analyzed by PHITS to obtain the shielding grid radius. The geometric parameters obtained by calculation and simulation were used to calculate the electric field distribution in ANSYS.
- (2) ANSYS modeling: The geometry, material properties, and applied voltages should be defined in ANSYS. The geometric parameters were obtained in the previous step. The dielectric constant of the gas medium and metal material that determines the material properties were set according to the user guide of ANSYS modeling for Garfield++. After adjusting voltages on the electrodes and the grid structure to a suitable value, the electric field distribution file required by Garfield++ can be outputted.

- (3) Energy resolution calculation: The electron drift velocity, diffusion coefficient, Townsend coefficient, and attachment coefficient, which are used to describe the drift characteristics of the electron, were calculated, and the results were exported to a file under certain gas conditions by using the Magboltz program. Files exported by ANSYS and Magboltz were inputted into Garfield++. For each gamma-ray detection event, the photon energy, interaction position, incident direction, and time of gamma-rays were set by using the Heed. Then, the position and time of gas ionization and the number of electron–ion pairs can be recorded, and the drift process of electron–ion pairs in the electric field can be simulated. The Signals program was used to set the recording time and time interval and recorded the current signal generated on the anode during the electronic drift. After setting the time constant τ of preamplifier and transfer function, the output current signal can be converted into a voltage signal. Once the amplitude of each output voltage signal has been recorded, the energy resolution can be obtained.

2.2. Detector modeling

Fig. 2 shows the structure of the HPXe cylindrical ionization chamber with a shielding grid. R_A , R_G , and R_C are the radii of the anode, grid, and cathode, respectively. L_C is the chamber length. T_C and T_G are the wall thickness and grid thickness, respectively. In the simulation of energy resolution, a point source is placed in the middle of the detector length, 5 mm away from the cathode in the chamber.

Among the parameters mentioned before, the setting of chamber length L_C , anode radius R_A , cathode voltage, and grid voltage directly refer to [1], wall thickness T_C , cathode radius R_C , grid radius R_G , grid thickness T_G , and time constant τ are optimized in the following simulation.

2.2.1. Optimization of the wall thickness T_C

The density of the gas is considerably lower than that of the scintillator or semiconductor; thus, filling the chamber with high-pressure gas is necessary to improve the detection efficiency. The wall thickness should be increased when increasing the gas pressure inside the chamber. However, the higher the wall thickness the more gamma-ray energy loss in the wall, which leads to a higher minimum detectable gamma energy [11]. The minimum detectable gamma energy mentioned in [11] and [1] are 20 and 100 keV, respectively; thus, 50 keV is selected in our simulations. Fig. 3 presents the percentage of absorbed gamma-rays in walls versus their energy for five values of vessel thickness (1, 2, 3, 4, and 5 mm of 304 stainless steel) calculated by PHITS.

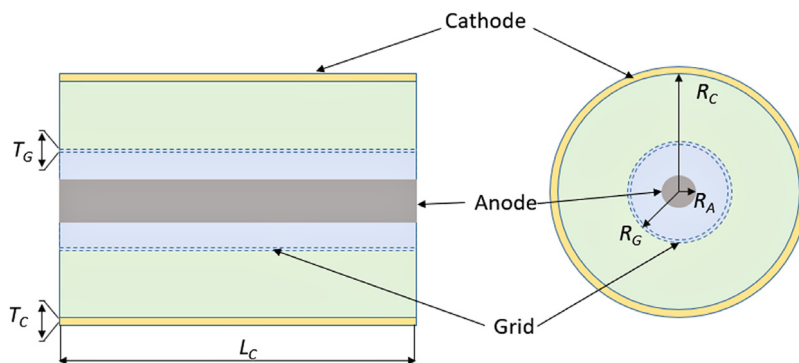


Fig. 2. Sketch of the HPXe ionization chamber for gamma spectrometry with a shielding grid.

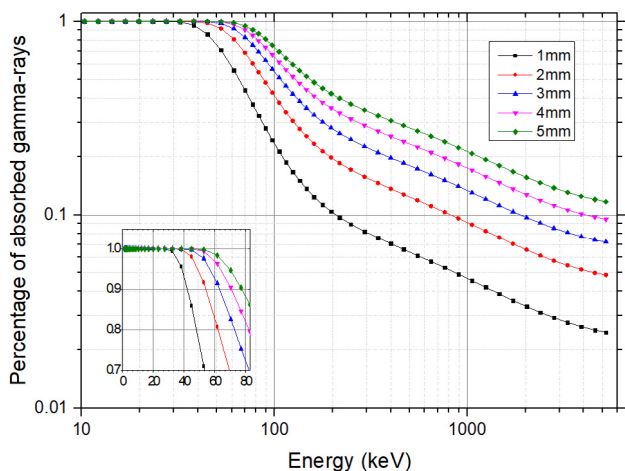


Fig. 3. Percentage of absorbed gamma rays in walls versus their energies calculated by PHITS.

The results are shown in Fig. 3 indicate that when the thickness of the stainless-steel wall was 1, 2, and 3 mm, the detector can detect 50 keV gamma-rays effectively. Structural strength needs to be considered in the chamber design, and the 3 mm stainless steel is selected in the simulations. Several researchers have studied the use of low-thickness stainless steel covered with a composite material, such as Kevlar, to improve the pressure resistance of the chamber [12]. This approach not only ensures an increased detection efficiency but also reduces the low energy limit of the detector. However, the material of the wall makes little influence on the following simulation of energy resolution.

2.2.2. Calculation of the cathode radius R_C

According to Chinese safety requirements for high-pressure seals, the pressure resistance of the detector shell must be greater than 1.5 times the actual working gas pressure. According to reference [11], the gas pressure is set to 50 bar in our simulation. When the shell thickness and gas pressure are determined, the cathode radius R_C can be calculated by using the following formula [13]:

$$R_c = \frac{\delta \times (2 \times \sigma \times \varphi - P)}{2 \times P} \quad (1)$$

where P is the pressure on the thin wall, which is set to 7.5 MPa (1.5 times the 50 bar); R is the radius of the pressure vessel; δ is the thickness of the thin wall, which is set to 3 mm; σ is the allowable tensile stress of the material, which is set to 137 MPa; φ is the average weld coefficient, which is set to 0.95. According to the formula, the cathode radius R_C is 50.56 mm. Referring to the HPXe gamma-ray spectrometer developed by MEPHI [1], the chamber length L_C is set to 250 mm, and the anode radius R_A is 5 mm. The total ionization chamber volume is approximately 2 L.

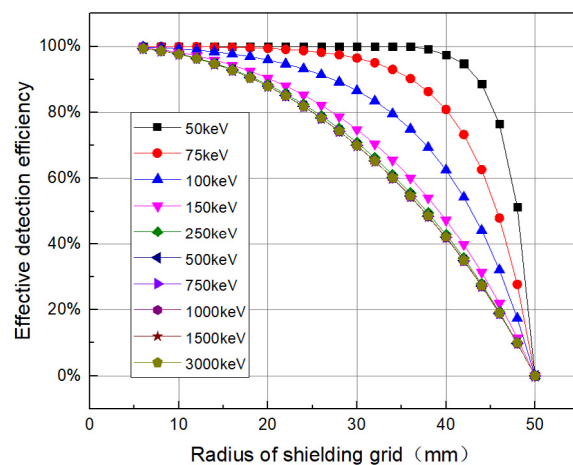


Fig. 4. Effective detection efficiency of HPXe gamma-ray spectrometer versus its shielding grid radius calculated by PHITS.

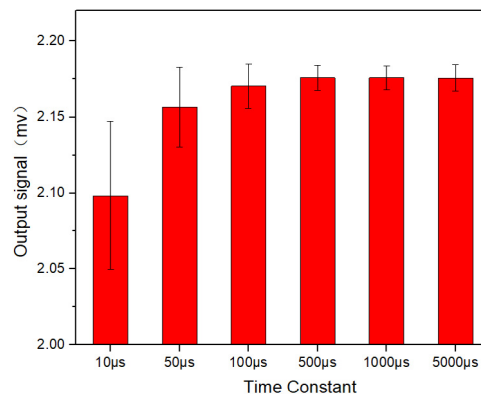


Fig. 5. Influence of the time constant on the output signal simulated by Garfield++.

2.2.3. Optimization of the grid radius

In the gridded ionization chamber, only the energy deposition event which happens in the cathode-grid space is effective [14]. To improve the effective detection efficiency, the volume ratio of the cathode-grid space in the chamber should be as large as possible. However, the anode-grid space cannot be excessively small due to a series of factors, such as processing difficulty and electric field uniformity. Fig. 4 shows the relationship between the effective detection efficiency and grid radius R_G under different gamma-ray energies calculated by PHITS.

As shown in Fig. 4, the effective detection efficiency decreases as the grid radius R_G increases. In addition, with the increase in gamma-ray energy, the percentage of deposition energy spent in the cathode-grid

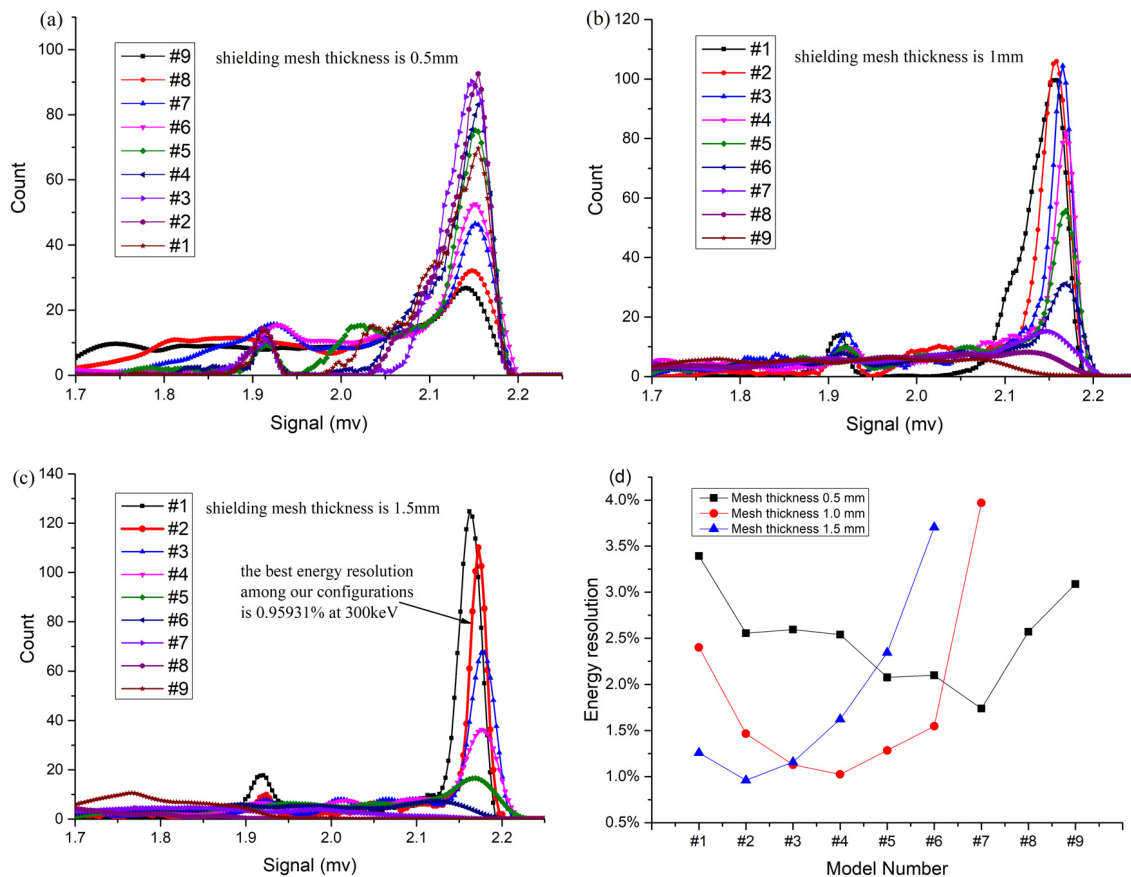


Fig. 6. Simulation of the spectrum of the output signal and energy resolution of HPXe gamma-ray spectrometer in each shielding grid structure: Shielding grid thickness: (a) 0.5 mm, (b) 1.0 mm, and (c) 1.5 mm. (d) Energy resolution.

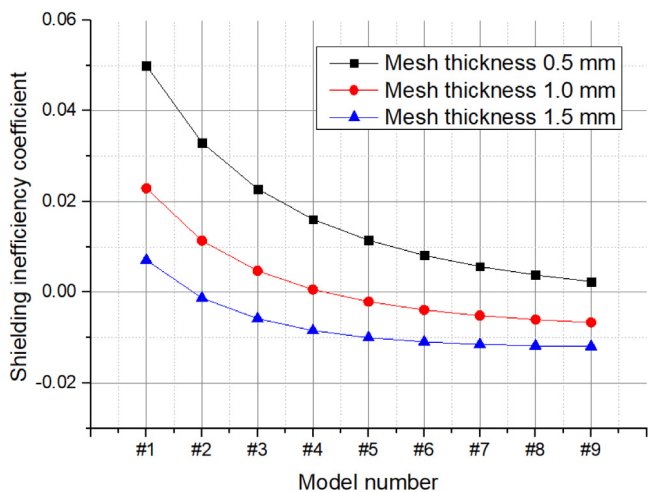


Fig. 7. Shielding inefficiency coefficient versus the shielding grid structure.

space tends to not depend on gamma-ray energy. Referring to the 88% effective detection volume of the HPXe detector mentioned in [15], the grid radius R_G is set to 18 mm in our simulations.

2.2.4. Electric field distribution modeling by using ANSYS

Based on the geometric parameter of the detector obtained in 2.2.1 and dielectric constants of the materials, a detector model can be constructed in ANSYS. According to the user guide of ANSYS modeling for Garfield++, the dielectric constants of gas medium and metal material

are set as 1 and 10^{10} respectively. Referring to the HPXe detector developed by MEPHI [1], the voltages of the electrodes are set as -20 kV, -12 kV, and 0 V for the cathode, grid, and anode, respectively. Then the file required by Garfield++ of the electric field distribution can be calculated and exported.

2.2.5. Optimization of the time constant τ

Magboltz calculates the drift characteristics of the electron under the certain gas condition. Referring to [1], we select 99.7% Xe and 0.3% H_2 with 50 bar pressure as the working gas. **The gas temperature is set to 293.15K which is close to room temperature in the simulation.** Gamma-ray energy can be set directly in HEED, and the range is 0 keV to 650 keV. 300keV is selected in the preliminary simulation.

In the HPXe spectrometer, the output current signal must be converted into the voltage signal through the electronic circuit before it is recorded. Convolution of the current signal and the transfer function is used to obtain the voltage signal during the simulation. The value of RC, namely, time constant τ , determines the voltage value of the charge integration in the electronic circuit.

Fig. 5 shows the voltage output signal under different time constants simulated by Garfield++. When the time constant is small, the output amplitude is low, and the statistic fluctuation of the output signal is poor. However, an excessively large time constant leads to a low counting rate. When the time constant reaches $500 \mu s$, the amplitude of the electronic output signal tends to be saturated, and the statistical fluctuation of the signal becomes relatively small. Hence, the simulated HPXe gamma-ray spectrometer obtains the best energy resolution. Besides, some of the existing HPXe detectors use the ORTEC 142AH preamplifier [16] with the same time constant of $500 \mu s$. The time constant is set to $500 \mu s$ in the following simulation.

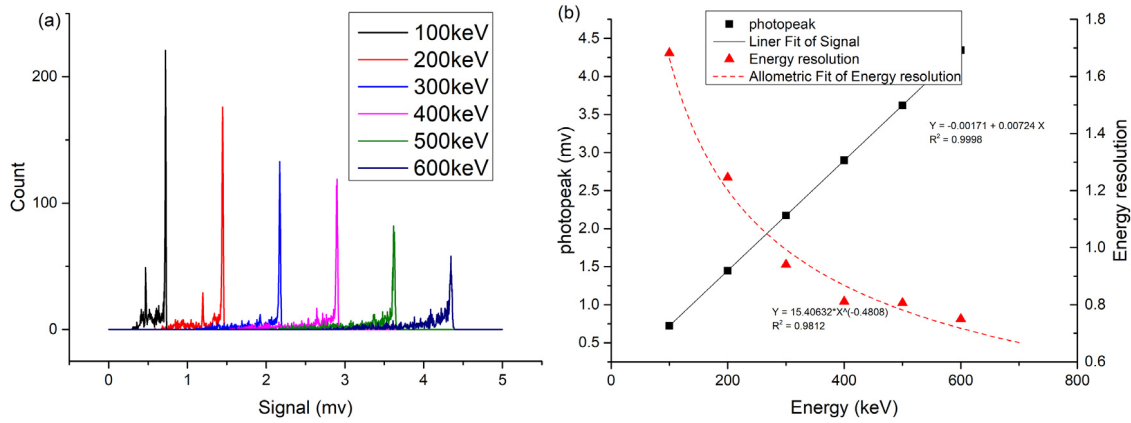


Fig. 8. Simulation of the output signal of HPXe detector response to the gamma-ray energy: (a) spectrum of the output signal (b) signal amplitude and energy resolution versus gamma-ray energy.

Until now, the model of HPXe gamma-ray spectrometer has been established. The output signals from Garfield++ can be used to calculate the energy resolution. The effect of critical parameters on the energy resolution will be discussed in the following section.

3. Result and discussion

3.1. Influences of grid structure on energy resolution

The change of the grid structure in the ionization chamber can affect the energy resolution [6]. The grid meshes are rectangles with an aspect ratio of 5:3 [1]. Three values of mesh thickness are set: 0.5, 1.0, and 1.5 mm. The grid has N wires stretched parallel to the anode, and the number of N ranges from 20 to 60. A total of 27 different grid structures are simulated, and Table 1 shows the designs.

The gamma-ray energy is set to 300 keV, the gas composition is 99.7% Xe and 0.3% H₂, and the gas pressure is set to 50 bar. Fig. 6 shows the spectrum of the output signal and the energy resolution under different shield grid structures. The total number of the count of each spectrum is 1800. The blocking of charge carriers by the grid wires is not considered in the simulation.

Fig. 6 presents that energy resolution varies greatly in different grid structures. When the mesh thickness is 1.5 mm, model #2, which has 25 wires stretched parallel to the anode, achieves the best energy resolution. When the mesh thickness is 1 mm, model #4, which has 35 wires, get the optimal energy resolution. The main reason is the shielding inefficiency of the shielding mesh [6]. In order to verify that the simulation results are consistent with the theory of shielding inefficiency, the shielding inefficiency is calculated by using the following formula:

$$\delta = (1/N) \ln(R_G/NR_0) / \ln(R_G/R_A), \quad (2)$$

where R_A and R_G are the radii of the anode and shielding grid, respectively. N and R_0 are the numbers of wires stretched parallel to the anode and the radius of wires, respectively, and R_0 is half of the mesh thickness T_G . Fig. 7 shows the shielding inefficiency of the shielding mesh under different cases of grid structures.

As shown in Figs. 6(d) and 7, the closer the shielding inefficiency of the shielding mesh to zero, the better the energy resolution. When the grid structure is #2 with a thickness of 1.5 mm, the best energy resolution 0.959% is obtained among the configurations we tried.

3.2. Energy resolution under different incident gamma-ray energies

The gamma-ray energy values are set to 100, 200, 300, 400, 500, and 600 keV to simulate the influence of energy resolution. The grid structure is model #2 with a thickness of 1.5 mm. As before, the gas

pressure is 50 bar, and the gas mixture is 99.7% Xe and 0.3% H₂; the total number of the count of each spectrum is 1800.

Fig. 8 shows the linear relationship between the energy and output signal and the dependence of the energy versus the energy resolution simulated by Garfield++.

As shown in Fig. 8(b), the linear fitting curve indicates that the output signal of the spectroscopic detector has a good linear correlation with the incident photon energy, and the linear correlation coefficient is 0.9998. On the basis of the fitting curve of energy resolution with the gamma-ray energy, when the energy is 662 keV, the energy resolution of the HPXe gamma-ray spectrometer is 0.678%. This value is close to the theoretical value, that is, 0.6% at 662 keV, mentioned in [4], and the deviation is 13.05%, which indicates the correctness of the simulation model.

3.3. Energy resolution under different gas compositions

In HPXe gamma-ray ionization chamber, it is very important to maintain the high purity of gas and a relatively high electron drift velocity to avoid charge carriers trapped. Several gas additives have been used in some gas detectors and successfully increase electron drift velocity in Xe, Ar, or other gas. In particular, H₂, CH₄, C₂H₅OH were used as gas additives in the HPXe ionization chamber [1], proportional counter [17], Geiger-Müller counter [14], respectively. In order to verify that the proposed method and simulation model can reflect the change of the signals with different gas compositions, the energy resolution under different gas compositions is calculated. The grid structure is model #2 with a thickness of 1.5 mm. The gamma-ray energy is 300 keV, and the gas pressure is 50 bar. The composition of air is 78%N₂, 21%O₂, 0.031%CO₂, 0.03%H₂O, and 0.939%Xe. The total number of the count of each spectrum is 1800. Fig. 9 shows the calculated energy resolution results.

As shown in Fig. 9, when the gas is composed of pure xenon, the energy resolution is 1.064%. By using 99.7% Xe and 0.3% H₂, the energy resolution is 0.959%; for 99.6% Xe with 0.3% H₂ and 0.1% C₂H₅OH, the energy resolution is 0.926%; for 99.7%Xe and 0.3%CH₄, the energy resolution is 0.903%. Besides, the position of the photopeak is kept at 2.1725 mV, which does not change with the addition of organic gas and polyatomic gas. When the Xe is mixed with H₂, CH₄, and C₂H₅OH, the reason for the improvement of energy resolution is that the organic gas and polyatomic gas can improve the drift characteristics of electrons in the ionization chamber [14], which is shown in Fig. 10(a). When 99.7% Xe and 0.3% H₂ are mixed with 0.01 ppm of air, the energy resolution worsens and 1.047% is obtained. When 99.7% Xe and 0.3% H₂ are mixed with 0.5 ppm of air, the signal is totally distorted. The shape and position of the photopeak changed in different degrees. The reason for the deterioration of signals when air is mixed can be found

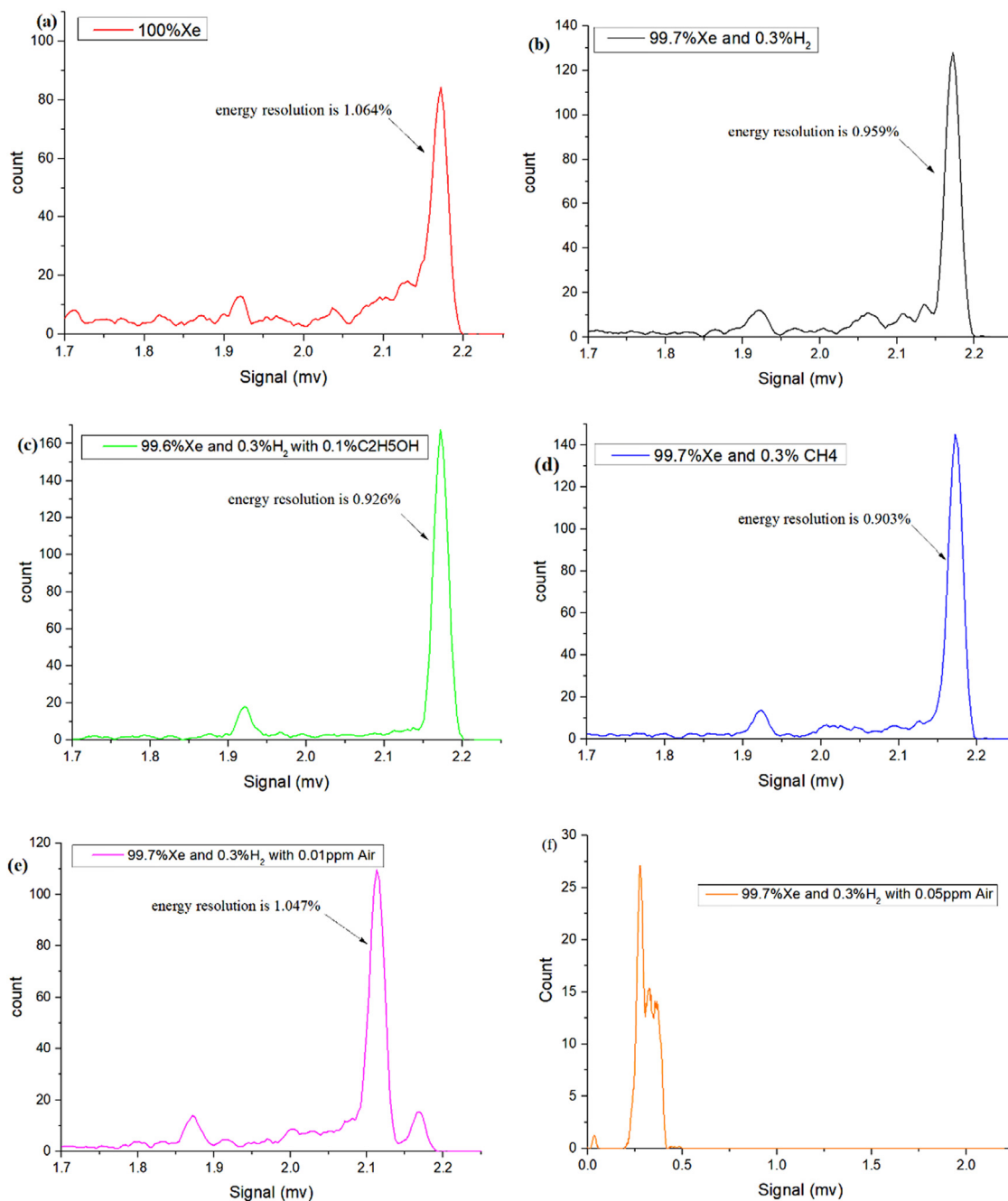


Fig. 9. Simulation of influence of gas composition on the energy resolution of HPXe gamma-ray detector.

Table 1 Geometrical parameters of mesh on the shielding grid.

Mesh No.	Number of wires stretched parallel to the anode	Mesh thickness (mm)	0.5	1.0	1.5
#1	20	Mesh size (mm)	7.80 × 5.20	7.05 × 4.70	6.30 × 4.20
#2	25		6.09 × 4.06	5.34 × 3.56	4.59 × 3.06
#3	30		4.95 × 3.30	4.20 × 2.80	3.45 × 2.30
#4	35		4.14 × 2.76	3.39 × 2.26	2.64 × 1.76
#5	40		3.53 × 2.35	2.78 × 1.85	2.03 × 1.35
#6	45		3.05 × 2.03	2.30 × 1.53	1.55 × 1.03
#7	50		2.67 × 1.78	1.92 × 1.28	1.17 × 0.78
#8	55		2.36 × 1.57	1.61 × 1.07	0.86 × 0.57
#9	60		2.10 × 1.40	1.35 × 0.90	0.60 × 0.40

in Fig. 10(b). The electronegative gas, such as oxygen, contained in the air increases the attachment coefficient, which increases the charge carrier trapping probability and affects signals collection. In Fig. 9(e),

on the one hand, due to the influence of electronegative gas, most of the amplitude of the signal of photopeak becomes smaller and forms the main peak. On the other hand, because of the small content of

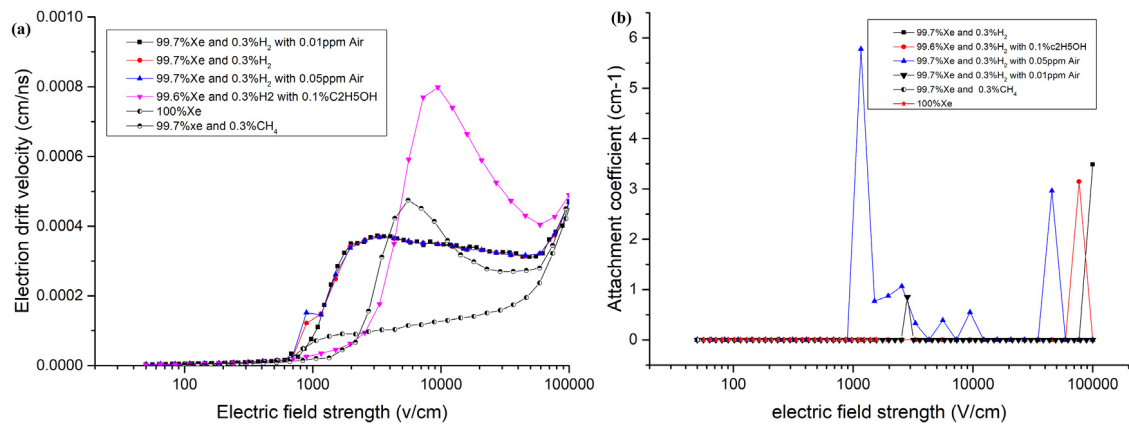


Fig. 10. Simulation of gas properties under different gas composition:(a) electron drift velocity versus electric field strength (b) attachment coefficient versus electric field strength.

electronegative gas, a small part of the signals does not get influenced and forms a small peak on the right of the main peak. In Fig. 9(f), because of the capture of most electrons in each signal, the photopeak amplitude gets reduced significantly and is close to the background. It is meaningless to calculate the energy resolution in this case.

4. Conclusion

In this study, a method combining PHITS, ANSYS, and Garfield++ was used to simulate the energy resolution of the HPXe gamma-ray detector. Geometric parameters were optimized by PHITS. ANSYS was used to calculate the electric field distribution. Signals produced by Garfield++ were used to calculate the energy resolution. The influence of critical parameters on energy resolution was discussed. The simulation results show that the variation of energy resolution with the grid structure is consistent with the variation in shielding inefficiency of the shielding grid. When the mesh thickness is 1.5 mm, and the number of wires stretched parallel to the anode is 25, the HPXe detector obtains the best energy resolution among the configurations we tried. Under this grid structure, the output signal of the spectroscopic detector has a good linear correlation with the gamma-ray energy. Besides, the simulation results show that the gas components have an influence on the signal. The introduction of electronegative gas in the working gas will cause signal distortion. Adding a little polyatomic gas can improve the drift characteristics of electrons and obtain better energy resolution. The deviation of energy resolution at 662 keV between our result and the expected theoretical value is 13.05%. The results prove the accuracy and feasibility of the proposed simulation method.

There are some limitations of this simulation; for example, the upper limit of the energy of gamma rays can only be set to 650 keV. These problems are expected to be solved in the following study.

CRediT authorship contribution statement

Jinchao Ma: Methodology, Software, Investigation, Writing - original draft, Supervision, Data curation. **Pin Gong:** Conceptualization, Validation, Investigation, Funding acquisition, Formal analysis. **Xi-aobin Tang:** Project administration, Supervision, Writing - review & editing, Funding acquisition. **Peng Wang:** Writing - review & editing, Data curation. **Wen Yan:** Software, Investigation, Methodology, Writing - review & editing. **Dajian Liang:** Supervision, Writing - review & editing. **Zeyu Wang:** Writing - review & editing, Investigation. **Rui Zhang:** Supervision, Writing - review & editing, Methodology. **Xiaolei Shen:** Writing - review & editing, Software.

Declaration of competing interest

The authors declare that they have no known competing financial interests or personal relationships that could have appeared to influence the work reported in this paper.

Acknowledgments

This work was supported by the National Natural Science Foundation of China (Grant No. 11675078), the Fundamental Research Funds for the Central Universities (Grant No. NT2020017), the Primary Research and Development Plan of Jiangsu Province, China (Grant No. BE2019727), the Funding of Jiangsu Innovation Program for Graduate Education, China (Grant No. KYLX16_0353).

References

- [1] V.V. Dmitrenko, S.E. Ulin, V.M. Grachev, K.F. Vlasik, Z.M. Uteshev, I.V. Chernysheva, K.V. Krivova, A.G. Dukhvalov, Perspectives of High Pressure Xenon Gamma-Ray Spectrometers to Detect and Identify Radioactive and Fissile Materials, in: NATO Sci. Peace Secur. Ser. B Phys. Biophys., 2008, pp. 155–172.
- [2] V.V. Dmitrenko, Vibrostability of high pressure xenon gamma-ray detectors, IEEE Trans. Nucl. Sci. 47 (2000) 939–943.
- [3] L. Gao, X. Tang, P. Gong, W. Yan, M. Ye, P. Wang, J. Zhang, Baseline restoration method based on mathematical morphology for high-pressure xenon detectors, Nucl. Instrum. Methods A 904 (2018) 163–170.
- [4] V.V. Dmitrenko, A.S. Romanyuk, S.I. Suchkov, Z.M. Uteshev, Compressed-Xenon Ionization Chamber for Gamma Spectrometry, Instruments Exp. Tech., New York, 1986, pp. 20–23.
- [5] A.E. Bolotnikov, V.V. Dmitrenko, I.V. Chernysheva, A.M. Galper, V.M. Gratchev, O.N. Kondakova, S.V. Krivov, S.I. Sutchkov, S.E. Ulin, Z.M. Uteshev, K.F. Vlasik, Y.T. Yurkin, Properties of compressed Xe gas as the detector medium for high-pressure Xe spectrometers, in: IEEE Nucl. Sci. Symp. Med. Imaging Conf. 1995, pp. 74–78.
- [6] A. Bolotnikov, B. Ramsey, Improving the energy resolution of high-pressure Xe cylindrical ionization chambers, IEEE Trans. Nucl. Sci. 44 (1997) 1006–1010.
- [7] R. Zhang, P. Gong, X. Tang, P. Wang, C. Zhou, X. Zhu, L. Gao, D. Liang, Z. Wang, Reconstruction method for gamma-ray coded-aperture imaging based on convolutional neural network, Nucl. Instrum. Methods A 934 (2019) 41–51.
- [8] K. Niita, T. Sato, H. Iwase, H. Nose, H. Nakashima, L. Sihver, PHITS-A particle and heavy ion transport code system, Radiat. Meas. 41 (2006) 1080–1090.
- [9] <http://www.ansys.com/>.
- [10] R. Veenhof, <http://cern.ch/garfield/files>.
- [11] A.S. Novikov, S.E. Ulin, I.V. Chernysheva, V.V. Dmitrenko, V.M. Grachev, D.V. Petrenko, A.E. Shustov, Z.M. Uteshev, K.F. Vlasik, Xenon gamma-ray detector for ecological applications, J. Appl. Remote Sens. 9 (2015).
- [12] R.L. Conder, N.L. Newhouse, Cyclic pressure test of a filament-wound vessel containing liquid nitrogen, Cryogenics (Guildf) 20 (1980) 697–701.
- [13] T. Tresca, H. Ze, Z. Jin, L.I.U. Peng, M. Cun, S.H.I. Jian, Discussion on thickness formula of cylindrical shell under internal pressure, Press. Vessel Technol. (2012) 18–21, (in Chinese).
- [14] Glenn F. Knoll, Radiation Detection and Measurement, John Wiley & Sons, 2010.
- [15] S.N. P'ya, K.F. Vlasik, V.M. Grachev, V.V. Dmitrenko, A.S. Novikov, D.V. Petrenko, A.E. Shustov, Z.M. Uteshev, S.E. Ulin, I.V. Chernysheva, Simulation of the xenon gamma spectrometer for analyzing radioactive materials, Bull. Lebedev Phys. Inst. 41 (2014) 247–251.
- [16] A.O. Pudov, A.S. Abyzov, S.A. Sokolov, L.N. Davydov, A.V. Rybka, V.E. Kutny, S.I. Melnikov, G.A. Kholomyeyev, S.A. Leonov, A.A. Turchin, Measurements and modeling of charge carrier lifetime in compressed xenon, Nucl. Instrum. Methods A 892 (2018) 98–105.
- [17] H. Sakurai, B.D. Ramsey, Characteristics of a high-pressure gas proportional counter filled with xenon, Proc. SPIE 1549 (1991) 20–27.